

# EFFECTS OF TI-MO AND TI-NB COMPLEX ADDITIONS ON INTERPHASE PRECIPITATION IN LOW-CARBON STEELS

Hung-Wei Yen<sup>1</sup>, Ching-Yuan Huang<sup>2</sup> and Jer-Ren Yang<sup>1</sup>

<sup>1</sup>Department of Materials Science and Engineering  
National Taiwan University, Taipei, Taiwan

<sup>2</sup>Iron and Steel R&D Department  
China Steel Corporation, Kaohsiung, Taiwan

Keywords: Interphase Precipitation, Nanometer-sized Carbide, TEM, Thermal Simulation, Phase Transformation, Hardness, Niobium, Molybdenum, Titanium

## Abstract

The purpose of this research was to study the effects of Mo and Nb additions on interphase precipitation in titanium-alloyed low-carbon steels. Sheet spacing and inter-particle spacing of interphase-precipitated carbides were quantitatively measured and evaluated by transmission electron microscopy. Besides, to elucidate these results, the transformation rate of ferrite was measured by dynamic dilatometer. Addition of 0.2 wt%Mo, which increases the super saturation for carbide nucleation, can further refine the inter-particle spacing of carbides. The Vickers microhardness has been achieved in this Ti-Mo containing steel after isothermal heat treatment at 650 °C for 20 min. Addition of 0.04 wt%Nb had no strong effect on refining the inter-particle spacing further. The precipitation of (Ti,Nb)(C,N) in the present alloy system increased the ferrite growth rate. It is suggested that the ability to refine the carbide dispersion in this Ti-Nb steel could be optimized by reducing the carbon content. These results and discussions provide guidance for alloy design to attain strong ferrite in steels by producing dense interphase-precipitated nanometer-sized carbides.

## Introduction

Interphase precipitation (IP), leading to the sheeted dispersion of nanometer-sized, complex alloy carbides ( $M_1M_2C$ ), has been shown to provide remarkable strength via precipitation hardening in advanced low-carbon ferritic steels. By this method, JFE and China Steel recently reported their developments of ultrahigh-strength hot-rolled steel strip for automotive use [1,2]. In these steels, the precipitation strengthening due to the IP of nanometer-sized carbides was estimated to be approximately 300 MPa.

Several mechanisms have been proposed in the literature [3-8] to explain the evolution of IP carbides. The most acceptable one is the ledge mechanism; during the austenite-to-ferrite transformation, the carbides nucleate densely on the terrace planes of the ledged  $\alpha/\gamma$  interface. As the ledge trails a complete passage, another ledge moves over a new parallel interface, where the nucleation cycle begins again. This process can be repeated many hundreds of times in a particular austenite grain, thereby leading to the well-characterised form consisting of sheets of carbides with uniform sheet spacing, in a ferrite matrix. The ledge mechanism was proposed only for the semi-coherent interface associated with rational  $\alpha/\gamma$  orientation relationships (ORs) and it

leads to a planar carbide dispersion of IP (PIP). The recent study by Yen et al. [9] claimed that the ledge mechanism can occur on interfaces associated with both rational and irrational ORs, thus leading to PIP or curved IP with a regular spacing (Regular CIP). Hence, by the ledge mechanism, the resulting density and distribution of tiny carbides relies on two factors, (1) the precipitation kinetics of carbides on the terrace plane and (2) the austenite-to-ferrite transformation kinetics. Both factors can be affected by the chemical composition of the steel. In general, the alloying elements expected to affect the interphase precipitation reaction can be categorised into four groups [10]:

- (1) elements which have a strong affinity with carbon atoms to form carbides and encourage the ferrite transformation, e.g. vanadium, titanium, and niobium;
- (2) elements which have some affinity with carbon to form carbides but slow down the ferrite transformation, e.g. molybdenum, tungsten, and chromium;
- (3) elements which stabilise ferrite or austenite and greatly affect the kinetics of ferrite transformation, e.g. manganese, nickel, and silicon;
- (4) interstitial elements which directly participate in carbide or carbonitride formation and also determine the kinetics of ferrite transformation, e.g. carbon and nitrogen.

The scope of the present work is to investigate, by using advanced TEM, the roles of Mo and Nb additions on the distribution of IP carbides in Ti containing low-carbon steels. Molybdenum and niobium solutes have a strong retarding effect on the ferrite growth but they are also supposed to participate in the formation of IP carbides. The interconnection between quantitative TEM results and dilatometry curves can provide further understanding of the effects of alloying on IP carbides.

### Experimental Procedure

The present investigation involved three different steels and their chemical compositions are listed in Table I. A Ti-containing C-Mn-Si steel was selected as the reference material (**Steel A**). To study the synergistic effects of Ti-Nb and Ti-Mo additions, two other steels, having approximately the same base composition but alloyed with additions of 0.2 wt%Mo (**Steel B**) and 0.04 wt%Nb (**Steel C**), were also evaluated. All of the steels were prepared by vacuum melting, and then cast into 100 kg ingots with a thickness of 210 mm. The ingots were homogenised at 1200 °C for 2 h and then hot rolled in several passes, by 20% reduction per pass, to plates of 20 mm thickness. In the present work, all the heat treatments were carried out on a Dilatronic III RDP deformation dilatometer from Theta Industries, Inc.

Table I. Chemical Composition of Three Steels (in wt%)

	Fe	C	Si	Mn	Ti	Nb	Mo	S*	N*
<b>A</b>	Bal.	0.10	0.1	1.5	0.2	-	-	44	40
<b>B</b>	Bal.	0.10	0.1	1.5	0.2	-	0.20	44	40
<b>C</b>	Bal.	0.10	0.1	1.5	0.2	0.04	-	43	40

\*(ppm)

Before the preparation of dilatometer specimens, the pieces of steel were homogenised at 1250 °C for 3 days while sealed in a quartz tube containing argon, and subsequently quenched in water. All dilatometer specimens were taken from the quarter thickness position below the plate surface, and orientated along the rolling direction before final machining to 3 mm diameter cylindrical rods of 6 mm length. The work was to study the effects of Ti, Ti-Mo and Ti-Nb additions on the precipitation of carbides during isothermal transformation. The processing schedules performed in the dilatometer are given in Figure 1. The specimens were austenitised at 1200 °C for 3 min (in order to dissolve all of the carbides), then cooled to 650, 680 and 700 °C respectively, at a cooling rate of 20 °C/s and held at these temperatures for different times, (20 and 60 min), and finally quenched to room temperature at a cooling rate of 100 °C/s.

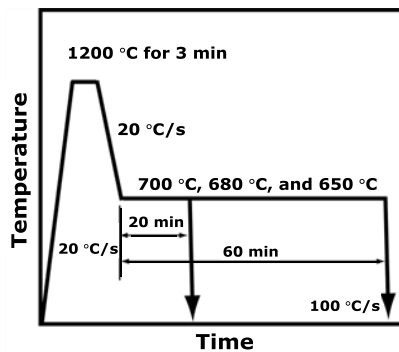


Figure 1. Schematic diagram of heat treatment process for isothermal transformation.

Optical metallography (OM) samples were prepared from the dilatometer specimens. The specimens were mechanically polished and then etched in 3% nital solution. For the purpose of revealing the precipitation hardening, hardness measurements were made on the ferrite phase in the optical specimens, using a Vickers hardness tester with a load of 100 g.

Transmission electron microscopy (TEM) samples were prepared from 300 µm thick discs slit from the dilatometer specimens. The discs were thinned to 60 µm by abrasion on SiC sandpaper and then electropolished in a twin jet electropolisher using a solution of 5% perchloric, 25% glycerol, and 70% ethanol at -20 °C and 35 V potential. The specimens were examined using a Tecnai G2 T20 TEM and FEI Tecnai F30 field emission gun TEM (FEG TEM). To measure the sheet spacing of IP carbides, a typical sheeted dispersion of carbides should be observed in TEM thin foils. Assuming the carbides precipitate on a terrace plane with index of  $\{h k l\}$  in the ferrite grain, to display an image of well-aligned interphase-precipitated carbides, the specified zone axes  $\langle u v w \rangle$  must satisfy the condition [3]:

$$hu + kv + lw = 0. \quad (1)$$

The zone axes satisfying Equation (1) will intersect the terrace plane edge-on and the typical sheeted distribution of carbides will be visible under these zone conditions. To estimate the inter-particle spacing, the foil thicknesses were measured by the log-ratio method for analysing the corresponding electron energy loss spectrum (EELS), which was collected with a semi-collection angle of about 19.4 mrad in TEM mode, using the mean free path in iron of 108 nm for inelastic scattering of iron [3].

## Results and Discussion

### Phase Transformation of Ferrite

After the isothermal heat treatments for 20 min, two phases are observed using OM, (1) diffusional ferrite, which nucleated and grew during the isothermal transformation and (2) martensite, which originated from the rapid cooling of untransformed austenite. The volume fraction and grain size of ferrite in the three steels after the isothermal heat treatments for 20 min are listed in Table II. The volume fraction of ferrite is apparently lower in **Steel B**, which implies a strong retarding effect of molybdenum on the ferrite transformation kinetics though molybdenum also participates in the formation of IP. As illustrated by the example in Figure 2, the ferrite grain size is finer in **Steel C**. Moreover, the ferrite grain size displays a clear bimodal distribution as shown in Figure 2(c), because the precipitation of (Ti,Nb)(C,N) in austenite enhances the nucleation rate of ferrite.

After the holding time of 60 min, the volume fractions of ferrite remain nearly the same in the three steels (i.e. 0.76 in **Steel A**, 0.78 in **Steel B**, and 0.75 in **Steel C** at 680 °C). The corresponding dilatometric curves for the isothermal transformations at 680 °C in the three steels have been analysed and are presented in Figure 3. It is worth noting that in the early stages the transformation rate of austenite in the Ti-Mo steel is dramatically lower than in the Ti and Ti-Nb steels. The slope of the linear portion of the transformation curve is lowest in **Steel B** and steepest in **Steel C** which means that the ferrite growth rate in **Steel B** was reduced. In this research, this effect is attributed to the retarding effect of molybdenum solutes on the interface mobility [11,12]. Niobium also has been reported to retard ferrite growth [13] but in **Steel C** this effect was not apparent. Instead, the ferrite transformation rate increases due to the addition of 0.04 wt% of Nb, compared with **Steel A**. The results from the dilatometer are consistent with the OM observations.

Table II. Volume Fraction and Grain Size of Ferrite in Three Steels Isothermally Heat Treated at Different Temperatures for 20 min

Vol. %	650 °C	680 °C	700 °C
<b>Steel A</b>	74(4)%	68(5)%	64(3)%
<b>Steel B</b>	66(5)%	58(6)%	47(6)%
<b>Steel C</b>	76(7)%	70(6)%	61(3)%
Grain size (µm)	650 °C	680 °C	700 °C
<b>Steel A</b>	48(9)	75(7)	92(9)
<b>Steel B</b>	43(10)	70(5)	87(11)
<b>Steel C</b>	28(12)	40(14)	71(9)

\*The value in () is the standard deviation of the measurement

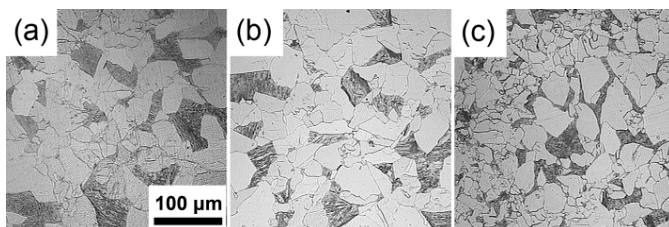


Figure 2. Optical micrographs taken from specimens; (a) **Steel A**, (b) **Steel B** and (c) **Steel C** isothermally treated at 680 °C for 20 min.

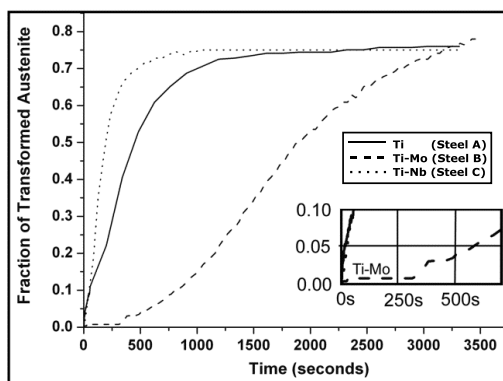


Figure 3. The isothermal transformation curves of three steels isothermally treated at 680 °C.

#### Interphase-precipitated Carbides in Ferrite

The distribution of interphase precipitated carbides is associated with two parameters, (1) the sheet spacing, the average distance between two neighbouring sheets of line-aligned carbides, and (2) inter-particle spacing, the average distance between two particles on the same sheet plane. To measure the sheet spacing, TEM images with exactly aligned sheets of carbides should be examined along some specified zone axes of ferrite grain as indicated by Equation (1). To obtain the inter-particle spacing, the thicknesses of specimens are measured by the log ratio method from EELS. This method provides higher accuracy, compared with some previous reports [14]. Typical TEM micrographs displaying sheeted carbides in each sample are shown in Figure 4. The sheet spacing and inter-particle spacing of the three steels, isothermally treated at 650, 680 and 700 °C for 20 min, are listed in Table III. Based on these results, three facts can be highlighted. Firstly, both sheet spacing and inter-particle spacing are refined with decreasing isothermal treatment temperature, with the variation of sheet spacing with temperature change being more dramatic. Secondly, the selection of carbide forming element itself can have a strong influence on the inter-particle spacing. It is apparent that the inter-particle spacing in **Steel B**

shows the finest distribution. Thirdly, on the other hand, the sheet spacing is not significantly affected by the selection of the carbide forming element in the present alloys.

Table III. Sheet and Inter-particle Spacing of the Three Steels Isothermally Treated at Different Temperatures for 20 min

	Sheet Spacing (nm)		
	650 °C	680 °C	700 °C
<b>Steel A</b>	19.6(6.0)	29.4(5.5)	40.6(7.3)
<b>Steel B</b>	19.1(5.6)	30.3(7.0)	38.8(10.1)
<b>Steel C</b>	18.5(4.4)	27.2(5.8)	36.9(12.4)
	Inter-Particle Spacing (nm)		
	650 °C	680 °C	700 °C
<b>Steel A</b>	38.7(8.8)	43.3(11.7)	48.6(12.0)
<b>Steel B</b>	33.4(11.2)	36.7(10.3)	43.9(15.2)
<b>Steel C</b>	40.4(8.8)	47.2(9.8)	53.3(11.9)

\*The value in () is the standard deviation of the measurement

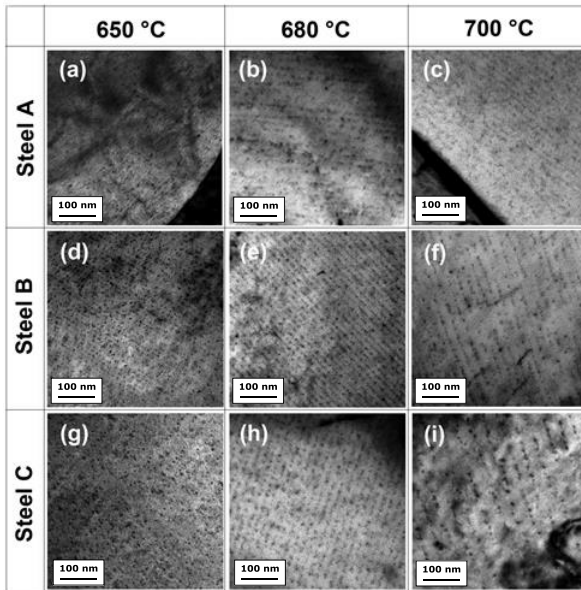


Figure 4. TEM micrographs showing the IP nanometer-sized carbides in the three steels isothermally heat treated at different temperatures for 20 min.

### Effects of Mo and Nb on Interphase Precipitation

The discussion here is based on the dilatometer experiments, OM observations, and TEM investigations. It follows the recent proposition that most interphase precipitation events in low-carbon steels occur via the ledge mechanism during austenite-to-ferrite phase transformation [9]. In **Steel B**, it is clear that the relatively slow growth rate during phase transformation is due to the retarding effect of molybdenum solutes. The slower ledge velocity could contribute to finer inter-particle spacings because of more time for (Ti,Mo)C to nucleate on the terrace planes. Furthermore, compared with **Steel A**, adding 0.2 wt%Mo can raise the supersaturation for carbide nucleation. It has been confirmed that molybdenum can participate in the MC-type carbide reaction [15]. Niobium solutes have also been reported to retard the ferrite transformation [13]. In **Steel C**, the retarding effect of niobium solutes was not observed. If niobium atoms precipitate as (Ti,Nb)(C,N), it can enhance the nucleation of ferrite and the ferrite transformation as shown in Figure 3. Although the remaining niobium solutes still participate in the IP reaction, the rapid ferrite transformation reduces the amount of carbide formation. Therefore, to optimise the carbide density in Ti-Nb containing steels, the carbon and titanium content should be reduced to suppress the niobium consumption due to the precipitation of carbonitrides. However, a reduction of Ti will lead to a reduction of the total amount of carbide formation. In the present alloy systems (with 0.1 wt%C and 0.2 wt%Ti), molybdenum does not tend to participate in the carbide reaction at high temperatures (i.e. >900 °C) even though the alloy contains 0.2 wt%Mo.

### Vickers Microhardness of Ferrite

The Vickers microhardness of ferrite has been measured for samples of the three steels, which have been isothermally treated at 650, 680 and 700 °C for 20 min, (using short holding times to prevent the coarsening of carbides), as shown in Figure 5. In the present conditions, the highest Vickers microhardness (301 HV) was obtained in **Steel B** isothermally transformed at 650 °C. The corresponding microstructure possesses the best combination of finest sheet spacing and finest inter-particle spacing as shown in Figure 4 and Table III. Such a high hardness of coarse-grained ferrite approximates to a yield stress of over 900 MPa. For this reason, it was defined as super ferrite [14]. In **Steel C**, heat treated at 650 °C for 20 min, a Vickers microhardness of 275 HV was also achieved with only a 0.04 wt% addition of Nb.

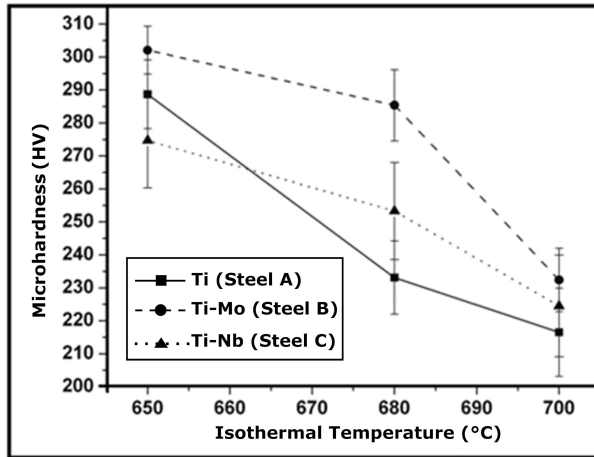


Figure 5. Vickers microhardness of three steels isothermally heat treated at 650, 680 and 700 °C for 20 min.

### Conclusions

The effects of Mo and Nb additions on interphase precipitation in three experimental Ti-containing steels have been quantitatively examined by advanced TEM techniques. The following conclusions can be drawn:-

1. Both sheet spacing and inter-particle spacing are refined with decreasing isothermal treatment temperature, though the sheet spacing changes more significantly with temperature.
2. Molybdenum has the advantage of producing more IP nanometer-sized carbides due to its efficiency in suppressing the ferrite transformation rate.
3. Due to the synergistic effects of Ti-Mo additions, the highest Vickers hardness of 301 HV can be achieved in coarse-grained ferrite after isothermal transformation at 650 °C.
4. Niobium in the present alloy accelerates the ferrite transformation due to the precipitation of (Ti,Nb)(C,N), such that it loses the potential to refine inter-particle spacing by the solute retarding effect on ferrite growth.
5. To optimise the carbide density, it is suggested to reduce the carbon content, such that the ability of niobium solutes to interact with the moving interface can be recovered.

### Acknowledgement

This work was carried out with financial support from the National Science Council of the Republic of China, Taiwan, under Contract NSC 98-2221-E-002-055-MY3. The authors thank China Steel Corporation for providing the alloy steels.

### References

1. Y. Funakawa et al., "Development of High Strength Hot-rolled Sheet Steel Consisting of Ferrite and Nanometer-sized Carbides," *Iron and Steel Institute Japan International*, 44 (11) (2004), 1945-1951.
2. C.Y. Huang et al., "Development of Nano-size Precipitation Strengthening Hot-rolled Automobile Steels" (Paper presented at the AISTech 2010 Iron and Steel Technology Conference, Pittsburgh, PA, 3-6 May 2010), 849-857.
3. R.W.K. Honeycombe, "Transformation from Austenite in Alloy Steels," *Metallurgical Transactions A*, 7 (7) (1976), 915-936.
4. R.A. Ricks and P.R. Howell, "Bowing Mechanism for Interphase Boundary Migration in Alloy Steels," *Metal Science*, 16(6) (1982), 317-322.
5. R.A. Ricks and P.R. Howell, "The Formation of Discrete Precipitate Dispersions on Mobile Interphase Boundaries in Iron-base Alloys," *Acta Metallurgica*, 31 (6) (1983), 853-861.
6. P.R. Howell, R.A. Ricks, and R.W.K. Honeycombe, "The Observation of Interphase Precipitation in Association with the Lateral Growth of Widmanstätten Ferrite," *Journal of Materials Science*, 15 (2) (1980), 376-380.
7. R.M. Smith, and D.P. Dunne, "Structural Aspects of Alloy Carbonitride Precipitation in Microalloyed Steels," *Materials Forum* (11) (1988) 166-181.
8. D.V. Edmonds and R.W.K. Honeycombe, *Precipitation Processes in Solids*, ed. K.C. Russell and H.I. Aaronson, (New York, NY: The Metallurgical Society of AIME, 20-21 September, 1976).
9. H.W. Yen et al., "Interphase Precipitation of Nanometer-sized Carbides in a Titanium-molybdenum-bearing Low-carbon steel," *Acta Materialia*, 59 (16) (2011), 6264-6274.
10. R.W.K. Honeycombe, *Structure and Strength of Alloy Steels*, (London, UK: Climax Molybdenum Company, 1975).
11. G.J. Shiflet and H.I. Aaronson, "Growth and Overall Transformation Kinetics Above the Bay Temperature in Fe-C-Mo Alloys," *Metallurgical Transactions A*, 21(6) (1990), 1413-1432.

12. W. Reynolds et al., "The Incomplete Transformation Phenomenon in Fe-C-Mo Alloys," *Metallurgical Transactions A*, 21 (6) (1990), 1433-1463.
13. M. Suehiro, Z.K. Liu, and J. Agren, "Effect of Niobium on Massive Transformation in Ultra Low Carbon Steels: A Solute Drag Treatment," *Acta Materialia*, 44 (10) (1996), 4241-4251.
14. H.W. Yen, C.Y. Huang, and J.R. Yang, "The Nano Carbide Control: Design of Super Ferrite in Steels," *Advanced Materials Research*, 89-91 (2009) 663-668.
15. H.W. Yen, C.Y. Huang, and J.R. Yang, "Characterization of Interphase-precipitated Nanometer-sized Carbides in a Ti-Mo-bearing Steel," *Scripta Materialia*, 61 (6) (2009), 616-619.